https://doi.org/10.5194/egusphere-2025-4561
Preprint. Discussion started: 13 October 2025

CarboKitten.jl – an open source toolkit for carbonate stratigraphic modeling

Johan Hidding[1], Emilia Jarochowska[2], Niklas Hohmann[2], Xianyi Liu[2], Peter Burgess[3], and Hanno Spreeuw[1]

[1]Netherlands eScience Center, Science Park 402 (Matrix THREE), 1098 XH Amsterdam, the Netherlands
[2]Utrecht University, Faculty of Geosciences, Princetonlaan 8a, 3584 CB Utrecht, The Netherlands
[3]University of Liverpool, School of Environmental Sciences, 4 Brownlow Street, Liverpool, L69 3GP, United Kingdom

Correspondence: Johan Hidding (j.hidding@esciencecenter.nl) and Emilia Jarochowska (e.b.jarochowska@uu.nl)

Abstract.

Stratigraphic forward modeling is a powerful tool for testing hypotheses about the geological record and conduct numerical experiments in stratigraphy at timescales not accessible to human observation. Open Source software for stratigraphic modeling available so far has focused on siliciclastic or terrestrial depositional environments. We present CarboKitten, a stratigraphic forward modeling toolkit for carbonate platforms. With performance and accessibility in mind, CarboKitten is implemented in Julia, using the literate programming approach.

CarboKitten integrates three components: the carbonate production model of Bosscher and Schlager (1992), the cellular automaton for spatial heterogeneity introduced by Burgess (2013), and a novel finite difference transport model inspired by Paola et al. (1992). The model simulates carbonate production through multiple biological factories (typically euphotic, oligophotic and aphotic), accounts for ecological processes that create spatial facies patterns through cellular automaton rules, and implements sediment transport via an active layer approach where material moves along paths of steepest descent.

Key features include support for different boundary conditions, variable sea level and insolation inputs, wave-induced transport capabilities, and visualization tools aiming at beautiful plots. The software exports data in the interoperable HDF5 format and includes functions for creating stratigraphic cross-sections, chronostratigraphic diagrams, topographic maps, and sediment accumulation curves. Performance benchmarks demonstrate linear scaling with grid size and time steps, enabling efficient execution on consumer hardware.

CarboKitten addresses a gap in available carbonate modeling tools by providing an accessible, well-documented, and modifiable toolkit for hypothesis testing in carbonate stratigraphy. The model operates on timescales from centuries to millions of years and can simulate various scenarios including orbital forcing, sea level change, and biological succession patterns. CarboKitten's accessibility should encourage broader adoption of stratigraphic forward modeling in carbonate research and education, supporting hypothesis-driven approaches to understanding the structure of the geological record and reconstructing the history of the Earth from carbonate strata.

https://doi.org/10.5194/egusphere-2025-4561
Preprint. Discussion started: 13 October 2025

1 Introduction

Stratigraphic forward modelling is well established as a means of examining our understanding of the formation of stratal architectures (Burgess et al., 2001; Paterson et al., 2006; Schlager and Warrlich, 2009; Ding et al., 2019; Jean Borgomano et al., 2020; Liu et al., 2022), prediction, correlation and imputation of architectures from incomplete data (Warrlich et al., 2008; Masiero et al., 2021), and testing hypotheses on the structure of the geological record (e.g., Kemp et al., 2018; Masiero et al., 2020; Liu and Liu, 2021) and the preservation of proxies (Curtis et al., 2025), fossils (Holland, 2000; Hannisdal, 2006; Hohmann et al., 2024), or forcing mechanisms (Kemp et al., 2016; Kemp and Van Manen, 2019; Burgess et al., 2019). Owing to their economic interest, most such models are proprietary to exploration companies and their availability to researchers is limited. Some older models developed by researchers share the fate of many other research software packages and their maintenance ceases, e.g. when a project ends (Warrlich, 2000). It is not always possible to resuscitate such models, especially if documentation or license are lacking or code has not been shared (e.g., Strobel et al., 1989; Demicco, 1998; Barrett and Webster, 2017). As a result, the choice of stratigraphic forward models available to researchers at the moment is narrow and shifted towards siliciclastic (Hutton and Syvitski, 2008; Sylvester et al., 2024) or specifically fluvial depositional systems (Wild et al., 2019; Falivene et al., 2019), to the point that researchers may resort to these models to create simulations of carbonate sections (Zimmt et al., 2021).

Modeling carbonate depositional systems requires not only accounting for water and atmospheric processes, but also for the biological character of sediment production and dispersal. Ecological processes, such as facilitation, competition and dispersal, may on one hand confound the relationships between sediment composition and water depth (e.g. Granjeon and Joseph, 1999; Dyer et al., 2018; Weij et al., 2019) and, on the other hand, lead to creation of complex facies patterns under stable sea level conditions (Drummond and Dugan, 1999; Purkis et al., 2016; Xi and Burgess, 2022). Complex models accounting for it have been mostly developed for exploration, e.g. `Carbonate 3D` (Warrlich et al., 2002, 2008), `DIONISOS` (Granjeon and Joseph, 1999) and `Carbonate GPM` (Hill et al., 2009). Of research-driven models operating in more than one dimension, two include a wider range of depositional environment with carbonate production modules: `CARB3D+` (Paterson et al., 2006), `SedSimple` (Tetzlaff, 2023) and `Badlands` (Salles, 2016), including its Python interface `pyBadlands` (Salles et al., 2018), but due to their general focus these models do not account for the spatial heterogeneity driven by biological processes. Finally, `CarboCAT` (Burgess, 2013) is a research-driven 2D model dedicated to stratigraphic forward modeling of carbonate platforms, which includes a cellular automaton that approximates the spatial heterogeneity formed through ecological interactions between carbonate-producing organisms. `CarboCAT` has been used in multiple studies (e.g. Masiero et al., 2020; Xi and Burgess, 2022; Hohmann et al., 2024), but having been written in Matlab, it was not accessible to contributions from the entire scientific community. Based on the successful applications of `CarboCAT`, we set out to develop a new generation model with the following specifications:

1. it should be Open Source and it should be easy for researchers to understand the algorithm, which is a prerequisite to being able to contribute to it or modify it to one's needs,

2. it should allow for spatial heterogeneity of carbonate facies,

https://doi.org/10.5194/egusphere-2025-4561
Preprint. Discussion started: 13 October 2025

3. it should include a sediment transport algorithm operating on different carbonate facies and produces realistic results without decreasing the model's performance substantially,

4. it should allow exporting and plotting multiple types of data users may need, including slices through the model grid, age-depth models, sediment accumulation curves, and stratigraphic columns,

5. it should be performant, easy to parallelize, and platform-independent,

6. it should be well documented and easy to use at a level accessible to a geosciences student.

The above prerequisites led us to re-designing the original architecture of `CarboCAT` and implementing its successor in Julia. In this article we present CarboKitten, an efficient and accessible Open Source model for stratigraphic forward simulations of carbonate platforms.

2 Model

CarboKitten combines the carbonate production model by Bosscher and Schlager (1992), the cellular automaton from Burgess (2013), and a custom finite difference transport model inspired on an approach by Paola et al. (1992). We describe each of these components in detail in the following sections.

2.1 Quantities

Since the model describes the accumulation of sediment under a range of variable conditions, a short discussion of different measures in the vertical column is in order.

Subsidence rate Quantified as a rate σ in units of $\mathrm{m/Myr}$. The growth of sediment is only sustainable in scenarios where there is a steady subsidence. In our models we use a default value of $50\ \mathrm{m/Myr}$ (or $0.5\ \mathrm{mm/kyr}$). This parameter can be set by the users.

Initial topography The model starts at an initial topography $\eta_0(x) = \eta(x, t_0)$, consisting of impenetrable bedrock. A more complex topography can be provided as an input array, e.g. by running a previous model and extracting the height of sediment.

Topography The present topography $\eta(x, t)$ is given as the initial topgraphy plus any amount of sediment accumulated over time. In our definition of η we don't correct for subsidence (see also the definition for water depth below).

Relative sea level The relative sea level $R(t)$ is usually a function of time, given as an input parameter of the model.

Water depth The water depth is computed from the current topography, relative sea level and subsidence rate,

https://doi.org/10.5194/egusphere-2025-4561
Preprint. Discussion started: 13 October 2025

Table 1. Parameters for the production model of the three default carbonate factories.

Factory	g_m [m/Myr]	I_k [W/m^2]	k [m^{-1}]
Euphotic	500.0	60.0	0.8
Oligophotic	400.0	60.0	0.1
Aphotic	100.0	60.0	0.005

$$w(x,t) = R(t) - \eta(x,t) + \int_{t_0}^{t} \sigma \mathrm{d}t. \tag{1}$$

2.2 Carbonate Production

The general form of our production model follows that of Bosscher and Schlager (1992) (BS92). This model finds the sediment accumulation curve by integrating an ODE that outside of the model parameters only depends on the initial topography.

$$\frac{\partial \eta}{\partial t} = P(\eta), \tag{2}$$

where P is the sediment production in m/Myr,

$$P(w) = g_m \tanh\left(\frac{I_0 e^{-kw}}{I_k}\right), \tag{3}$$

where I_0 is the insolation, I_k is the saturation intensity, k the extinction coefficient and g_m the maximum growth rate.

This model encapsulates both the exponential extinction of sun light as water depth increases, and the idea that the growth of organisms interpolates between no growth at great depth and saturated growth in shallow waters (i.e. solar input is not the limiting factor at those depths).

Here we parametrize P as a function of w. Note that $\nabla w = -\nabla \eta$, but otherwise we'll use w and η wherever one or the other is more convenient.

Following Burgess (2013), we extend the BS92 model by introducing multiple facies that each have their own growth characteristics (except for insolation I_0, which is a global input variable).

$$P(w) = \sum_f P_f(w) \tag{4}$$

Our default parameters define three biological facies based on sediment produced by three carbonate factories: the euphotic (E), oligophotic (O) and aphotic (A)) factories. The default values for these factories are shown in Table 1, and the resulting production curves shown in Figure 1.

https://doi.org/10.5194/egusphere-2025-4561
Preprint. Discussion started: 13 October 2025

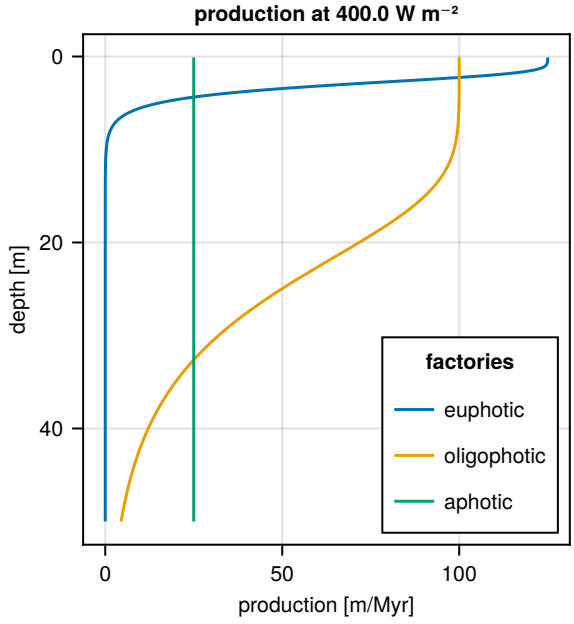

Figure 1. Production curves for three default carbonate factories

2.3 Cellular Automaton

The Celullar Automaton (CA) in CarboKitten is a direct reimplementation of the one described by Burgess (2013) in their package CarboCAT.

The CA emulates the biological succession of species by following a set of simple rules. If conditions are right, a species will multiply and occupy neighbouring territory. However, when there are too many of the same kind, the species will die from over population.

For each cell in the grid a centered neighbourhood of 5×5 pixels is considered. We count the number of neighbouring cells of the same species. Then we consider two ranges: the *activation range* (default $6 \leq n \leq 10$) and *viability range* (default $4 \leq n \leq 10$). If the number of live neighbours is in the viability range, the cell stays alive. If the cell was dead, but the number of live neighbours is in the activation range, the cell becomes alive.

Since a dead cell may qualify to become alive for different carbonate factories at the same time, birth priority is rotated every iteration.

In the default configuration we emulate three species, corresponding to the factory species discussed in the section on carbonate production. The state of the CA determines which carbonate factory is switched on for each cell in the grid.

https://doi.org/10.5194/egusphere-2025-4561
Preprint. Discussion started: 13 October 2025

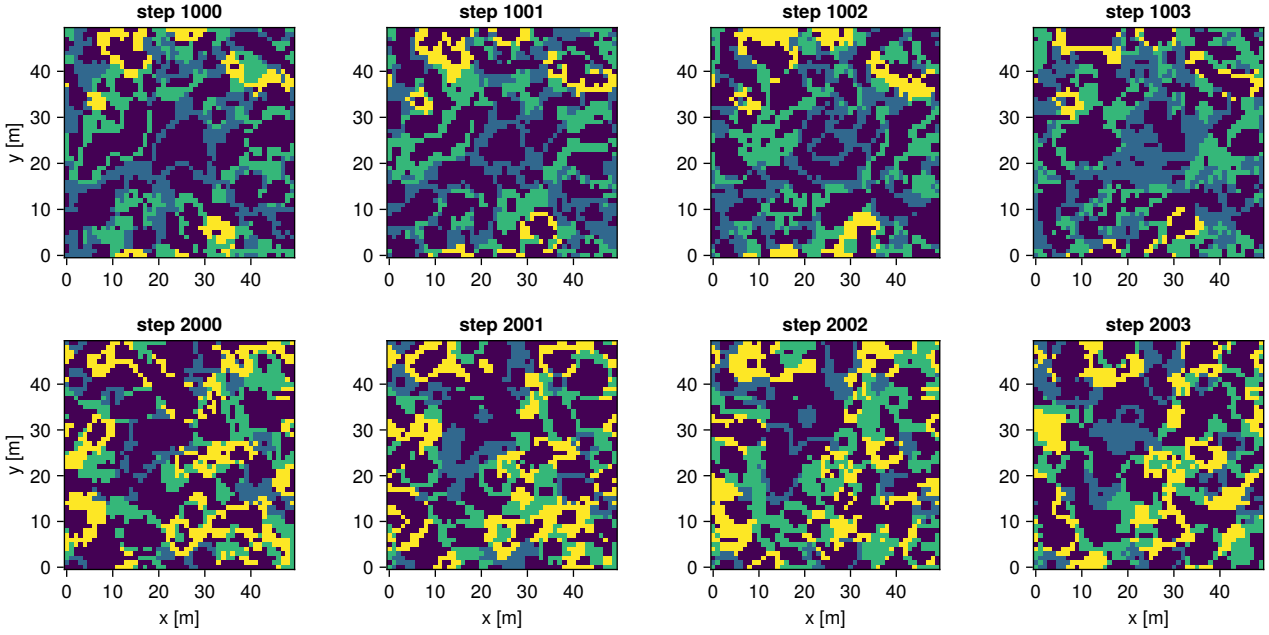

Figure 2. Iterations of the CA, as described by Burgess (2013), on a periodic grid of 50×50. Starting with random noise, we first iterate 1000 times to get into a typical state. The top row shows iterations 1000 to 1003, the bottom row 2000 to 2003. This shows that the patterns keep reasonably stable on the short term, while evolving more extensively over the long term.

2.4 Transport

Our transport model is borrowed from other similar approaches in siliclastic (river bed) modeling (See Paola et al., 1992; James et al., 2010), where it is made plausible that this approach is viable for models that work on long time scales. Because our transport model is novel (at least for modelling carbonate platforms), we discuss the full model in a separate section. Here, we discuss how transport is embedded in the larger model.

We consider all sediment transport to happen in an **active layer** close to the sea floor. This layer has a certain concentration of sediment C_f that travels along a path of steepest descent. We say that this material is **entrained**. Every time step the active layer is fed with freshly produced sediment and distintegrated older sediment. After transport a fraction of the entrained sediment is deposited on the sea floor in process that we refer to as **lithification**, being the process of turning loose sediment into rock. Although in reality sediment might not be mobile for a while before lithification sets in, for the purpose of our model, we chose the term to represent the immobilisation of sediment as a whole, see Figure 3.

The actual transport is computed using a finite difference approach that is further discussed in Section 3.

https://doi.org/10.5194/egusphere-2025-4561
Preprint. Discussion started: 13 October 2025

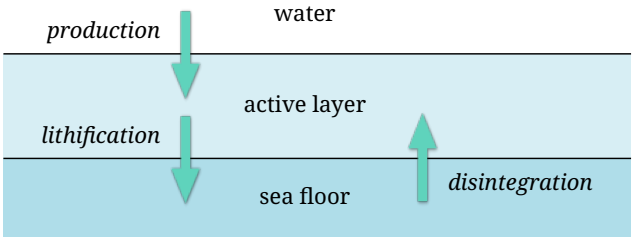

Figure 3. Diagram showing concepts of production, lithification and disintegration. Every time step newly produced sediment and older disintegrated material (configured as a disintegration rate) is added to the active layer. After transport, a set fraction of the sediment (configured as a lithification half-life time) is lithified, becoming the sea floor.

2.5 Composed model

Putting everything together, we evaluate the model as follows each iteration:

1. Advance the cellular automaton.
2. Compute the production P_f.
3. Disintegrate sediment D_f.
4. Transport entrained sediment C_f.
5. Deposit lithified sediment.

Advancing the CA can be configured to happen one-in-n iterations to slow it down. Transporting the sediment can be computed on smaller time steps if required for numeric stability.

2.6 Input parameters

CarboKitten has many input parameters: box geometry, time parameters, a list of facies properties, transport model intrinsics and external conditions: initial topography, relative sea level and insolation. We've already discussed the facies properties in Section 2.2, and the transport model is discussed in Section 3. That leaves us the external conditions that should be considered the driving forces of carbonate platform formation.

The initial topography, sea level and insolation can all be entered in three different ways: a given constant, a Julia function or an array exactly matching the box size or number of time steps.

In Section 5 We provide two examples where we use external sources to drive the sea level and insolation curves. A full list of input parameters is available in the Appendix.

https://doi.org/10.5194/egusphere-2025-4561
Preprint. Discussion started: 13 October 2025

2.7 Visualisations

CarboKitten generates data in the accessible, binary HDF5 format, thus output can be visualised with most common tools, e.g. imported into R or a Jupyter notebook. Nevertheless, we provide some routines based on Makie (Danisch and Krumbiegel, 2021) for creating crosssections, Wheeler diagrams and topographic overviews. Some of the most common plot types have been collected into a summary plot, which is shown in Figure 4.

3 Transport

In Section 2.4 we discussed how transport is embedded in the larger model. Our transport model supposes that all entrained sediment resides in a layer of constant thickness just above the sea floor, also known as the **active layer**. The concentration of sediment C_f is considered separately for each facies (as with all quantities with the f subscript). Each iteration of the larger model we supply the active layer with freshly produced (autochthonous) sediment as well as disintegrated older (allochthonous) sediment. We then compute transport of the active layer for as many sub-iterations as is deemed needed for the solver to remain stable. After that, a percentage of the contents in the active layer is deposited on the sea floor. The lithification percentage depends both on the time step taken and the given lithification time, which is configured in terms of a half-life time. There are many ways to compute sediment transport in the active layer. We've opted for a finite difference strategy inspired on Paola et al. (1992).

We assume a local sediment flux proportional to the local gradient,

$$\boldsymbol{q}_f = -C_f(d_f \boldsymbol{\nabla}\eta + \boldsymbol{v}_f(w)), \tag{5}$$

where d_f is a facies dependent diffusivity, and $v_f(w)$ is a chosen additional velocity as a function of water depth. Optionally, we use $v_f(w)$ to model wave induced sediment transport (for an example see Section 5.3). The mass balance (continuity equation) is then,

$$\frac{\partial C_f}{\partial t} = -\boldsymbol{\nabla} \cdot \boldsymbol{q}_f \tag{6}$$

This gives us an advection equation for the sediment concentraiton C_f. We also express everything in terms of water depth, having $\nabla w = -\nabla \eta$, arriving at

$$\frac{\partial C_f}{\partial t} = -(d_f \boldsymbol{\nabla} w + \boldsymbol{v}_f(w)) \cdot \boldsymbol{\nabla} C_f + (\boldsymbol{s}_f(w) \cdot \boldsymbol{\nabla} w - d_f \nabla^2 w) C_f, \tag{7}$$

where $\boldsymbol{s}_f(w) = \boldsymbol{v}_f'(w)$ is the velocity shear, or the derivative of the velocity with respect to water depth. We solve this PDE using a finite difference method-of-lines approach with an explicit solver (forward Euler and 4^{th} order Runge-Kuta are supported).

https://doi.org/10.5194/egusphere-2025-4561
Preprint. Discussion started: 13 October 2025

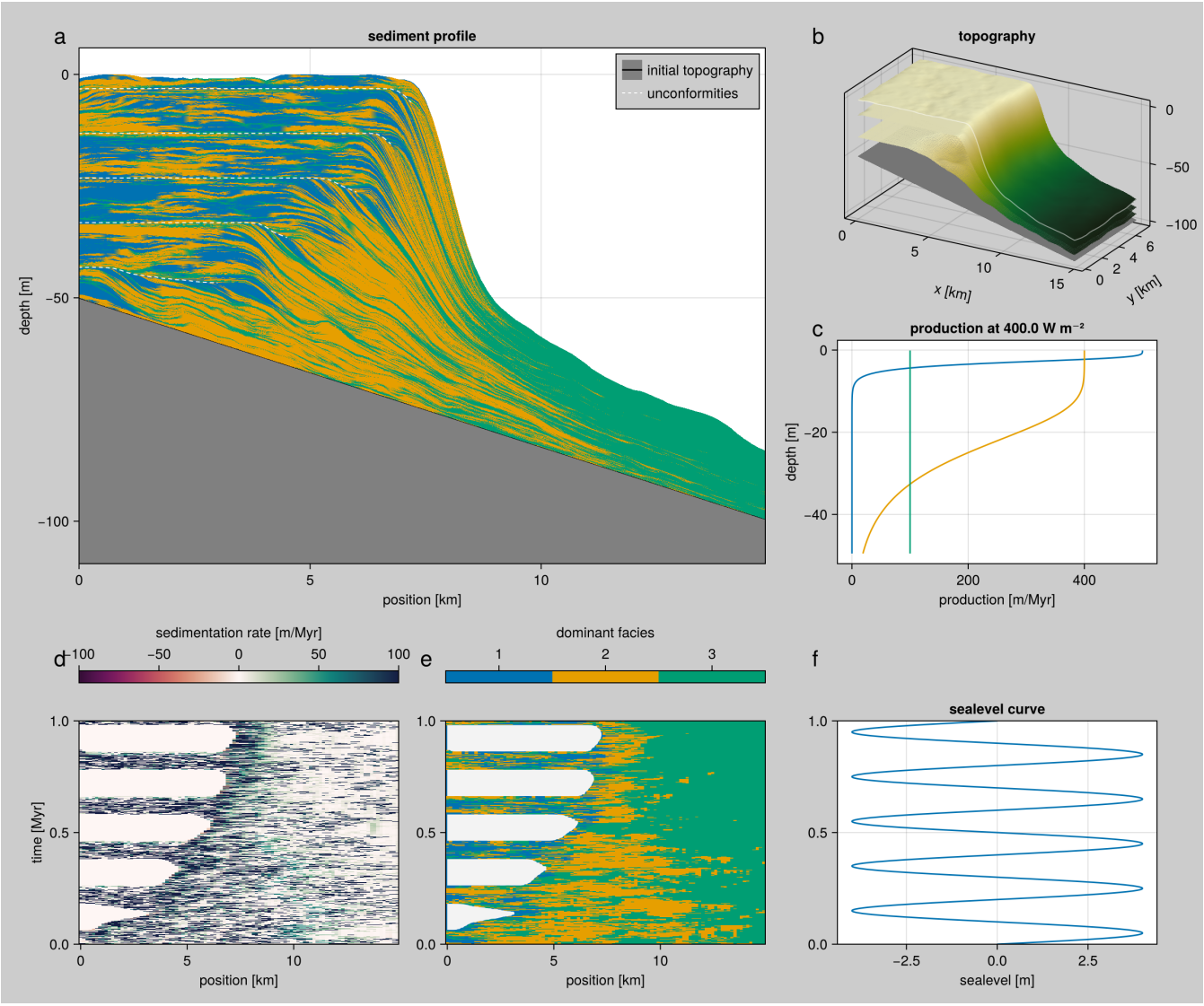

Figure 4. Overview of different visualizations supported by CarboKitten. Panel (a) shows a stratigraphic crosssection, including an indication for unconformities, (b) a topographic overview including two intermediate time steps, (c) the production curves used, (d) sedimentation rate as a function of time (Wheeler diagram), (e) dominant facies as a function of time, (f) the sea-level curve given as input. The combined plot is arranged such that spatial data is on the top row, while time-dependent information is shown at the bottom with matching y-axes.

https://doi.org/10.5194/egusphere-2025-4561
Preprint. Discussion started: 13 October 2025

Note that, although the transport equation is an advection equation in C_f, if we consider that C_f acts as a proxy for η through disintegration and lithification, what seems like an innocent reaction term in Equation 7, turns out to behave as a diffusion equation in η. This is why we refer to d_f as the *diffusion coefficient* of a particular facies. Any attempt at modelling sediment transport where there is an effective down-slope flux combined with some form of disintegration will yield diffusive behaviour.

3.1 Other approaches

In the critical angle approach developed by Warrlich (2000), sediment is transported from unstable slopes to the nearest down-slope stable region. Stability is defined separately for different grain sizes. This method is motivated by the empirical relationship between grain composition and maximum slope angle (Kenter, 1990).

The problem with this critical angle-based method of transport is that production across an unstable region is deposited on a small strip, where slopes are below the critical angle. It becomes unclear how to interpret these models from a physics point of view, as results depend heavily on the time-step that is chosen. Contrasting to that, both our transport model and production model (with the exception of the cellular automaton) are discretisations of otherwise continuous processes. This means that, at least assymptotically (i.e. as long as the time step is small enough), our implementation is independent of the chosen time step.

One aspect of critical angle theory that we do use is that we can modulate the disintegration rate (and therefore the amount of entrained material) with the magnitude of the slope $|\nabla\eta|$. If we only disintegrate material where the slope is supercritical, the net effect is that sediment is transported from supercritical to stable areas. The difference is that we have a much better control over the physics, and we don't need to convert back and forth between gridded values and a particle representation used in the critical angle approach (e.g. Warrlich, 2000).

A different approach has been used in the early model `CARBPLAT` by Bosscher and Southam (1992), which took empirically observed carbonate slopes (such as started by Kenter (1990) and studied by others, including Adams and Schlager (2000)) and defined a slope function that returned slope parameters bounded by the limits of the angle of repose. In this study an exponential slope function was assumed, although it should be noted that there is literature debate on the distribution of slope shapes of carbonate platforms (e.g., Schlager and Camber, 1986; Kenter, 1990; Adams and Schlager, 2000). This modelling approach is agnostic with respect to sediment properties and transport mechanisms and optimises the similarity to observed shapes, allowing the user to choose the parameter that produces the best result. However, it does not allow modelling a mixture of sediment types with different properties and requires an a priori assumption on the expected slope shape. It had not been adapted in subsequent models.

3.2 Parameter choices

Our transport model is based on the elementary assumption that sediment flux is proportional to the slope of the sea floor. Nevertheless, we are extrapolating this idea to time scales on which it is hard to reason or otherwise measure the parameters to our model. Especially the combination of diffusivity, disintegration rate and lithification time can be pivotal in acquiring a set

https://doi.org/10.5194/egusphere-2025-4561
Preprint. Discussion started: 13 October 2025

of physical outcomes, while we have no good way to estimate acceptable ranges of values for them, other than trying them out and see if the results are plausible.

3.2.1 Disintegration versus lithification

Both the disintegration rate and the lithification time modulate how long sediment resides in the active layer. By carefully scaling one or the other, the effective diffusion of material can be controlled without changing the specific diffusivity. However, choosing a high lithification time (thus a slow lithification) over a high disintegration rate can help in transporting only freshly produced sediments.

Note that not setting the lithification rate (which would amount to immediately depositing all of the active layer on every iteration) results in models that depend heavily on a chosen time step.

To understand the relative effects of choosing a certain lithification time and/or disintegration rate, we ran a one-dimensional model where sediment is produced in a central patch. Then we can study the rate at which sediment is dispersed, either by direct transport before lithification happens, or by subsequent disintegration and re-deposition. By carefully choosing the parameters, we can make a slow lithification process look very similar to a high disintegration rate, as shown in Figure 5.

3.3 Implementation and limitations

Our implementation of the transport model first computes the gradient of the sea floor (or equivalently the water depth) $\boldsymbol{\nabla} w$ using central differences. From this gradient we can compute the advection coefficients in Equation 7, $\boldsymbol{c}_{\text{adv}} = d_f \boldsymbol{\nabla}\eta + \boldsymbol{v}_f(w)$. The maximum advection coefficient sets the Courant number and determines how many time steps we need to take to solve Equation 7. For an advection equation integrated with the forward Euler method, we need

$$|c_{\text{adv}}|_\infty \frac{\Delta t}{\Delta x} \leq 1. \tag{8}$$

This states that we cannot move matter further than a single pixel distance in one iteration, or our computation becomes unstable. Since we can compute the transport coefficients in advance, it is relatively cheap to apply multiple iterations of the advection solver, for which we use an upwind scheme.

Now consider our transport model in the context of the larger carbonate platform model. Each time we disintegrate some matter which gets entrained and transported as part of the sediment concentration C_f, after which a fraction is cemented, increasing η. If we consider $\partial\eta/\partial t \sim \partial C/\partial t$, then part of the transport equation is the diffusion equation $\partial\eta/\partial t = d_f C_f \nabla^2 \eta$. This leaves our implementation vulnerable to instabilities when the global time step is taken too large. For just this diffusion term the CFL limit is

$$d_f C_f \frac{\Delta t}{(\Delta x)^2} \leq 1. \tag{9}$$

https://doi.org/10.5194/egusphere-2025-4561
Preprint. Discussion started: 13 October 2025

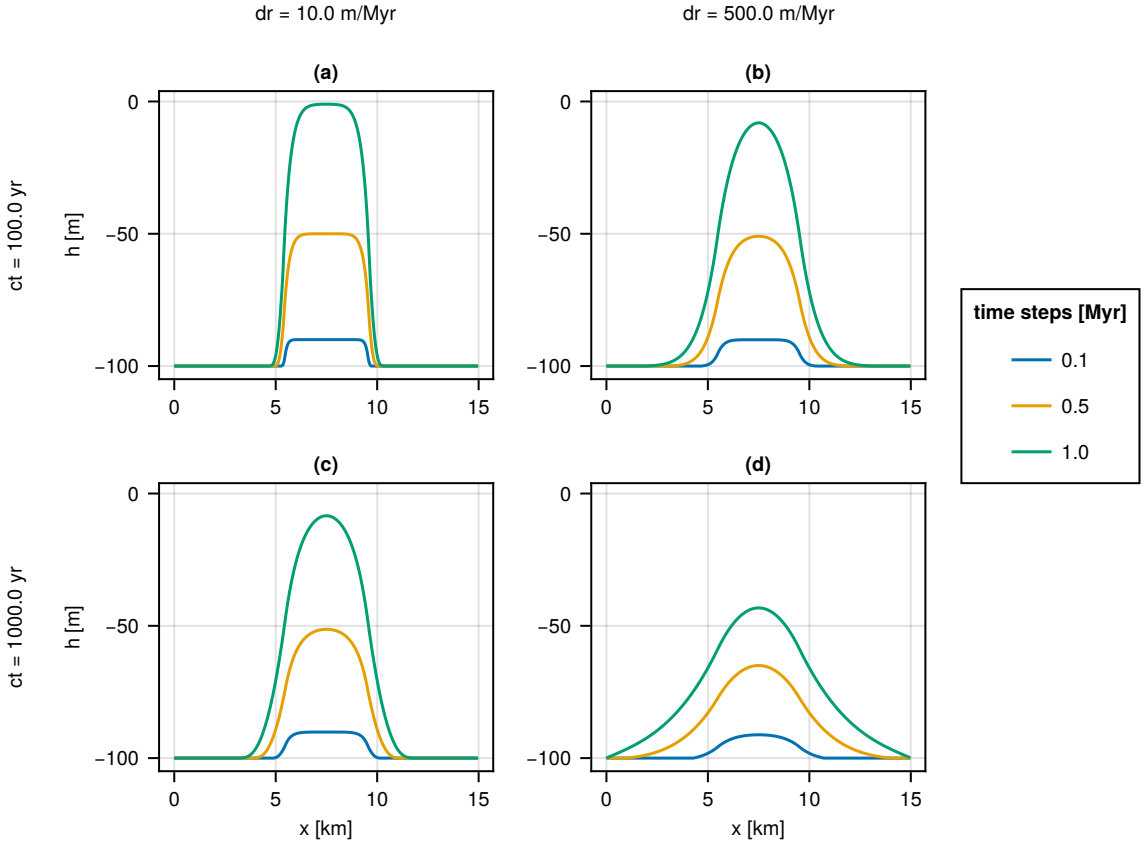

Figure 5. Comparison between lithification and disintegration. The four panes show different combinations of parameters for a one-dimensional model. We have enabled a production of 100 $\mathrm{m/Myr}$ for a 4 km wide patch in the middle of the box, and chose a runtime of 1 Myr with a time step of 100 yr (the sharp edges in the production profile induce fast transport, requiring small time steps), and the diffusivity was set to 10 $\mathrm{m/Myr}$. Panels (a) and (b) have a short lithification time `ct` (100 yr), while panels (c) and (d) have a long lithification time (1000 yr). On the columns, (a) and (c) have a low disintegration rate `dr` (10 $\mathrm{m/Myr}$), while (b) and (d) have a high disintegration rate (500 $\mathrm{m/Myr}$). Values were chosen to have a similar net effect on the dispersion of produced sediment.

https://doi.org/10.5194/egusphere-2025-4561
Preprint. Discussion started: 13 October 2025

This means that increasing the resolution of a model by a factor two, may need a time step four times smaller to remain stable. There are ways around this limitation, but our current aims to not necessitate the corresponding investment in development time.

4 Software design

4.1 Box topology

CarboKitten needs to work with different choices for box topology, i.e. how the boundaries of a model box connect to each other. For example, when we simulate a small strip of coastline it is best to have one axis (in this case the x-axis) reflect onto itself, while the other axis is periodic, leaving fewer edge effects.

In another case, where we want to simulate an entire island, or even an archipelago, it is more convenient to use fully periodic coordinates. We illustrate these choices in Figure 6.

4.2 The sediment buffer

In our models of sediment transport and denudation it is important to remember the sedimentation history for all produced facies for some time into the past. We keep a three-dimensional fixed-size buffer, where two dimensions represent the x and y coordinates of the system, and the third dimension discretizes the amount of deposited material. Each cell in the buffer represents a parcel of sediment, where we store the relative fractions of each contributing facies. We emphasise that this buffer is only used to determine the facies composition of disintegrated sediment. The sediment output of the overall model is written to disk at each iteration for post-analysis, but is no longer an active component in the model. This means that the model output can be much more precise than the depositional resolution of the buffer.

While the sediment buffer is allocated as a single 4-dimensional array (depth, facies, x, y), it is best to explain its functioning from the perspective of a single cell in our model. We are left with two dimensions: depth (rows) and facies (columns).

We choose to have the head of our sediment stack always be at the first row. When sediment out-grows the buffer, the deepest layers are dropped from memory. The head can contain an incomplete amount of sediment, while all rows below the head are either full or empty. When sediment is pushed to the stack and the head row overflows, all rows are copied down one row and the surplus is assigned to the now empty head row. The inverse happens when removing (popping) material from the stack. This process is illustrated below in Figure 7.

4.3 User interface

The user interfaces CarboKitten by writing a Julia script that defines the relevant model parameters and runs the chosen model. Effectively, very little Julia needs to be known to take an example input and modify parameters. Output is written to HDF5 files for post-processing and visualization.

https://doi.org/10.5194/egusphere-2025-4561
Preprint. Discussion started: 13 October 2025

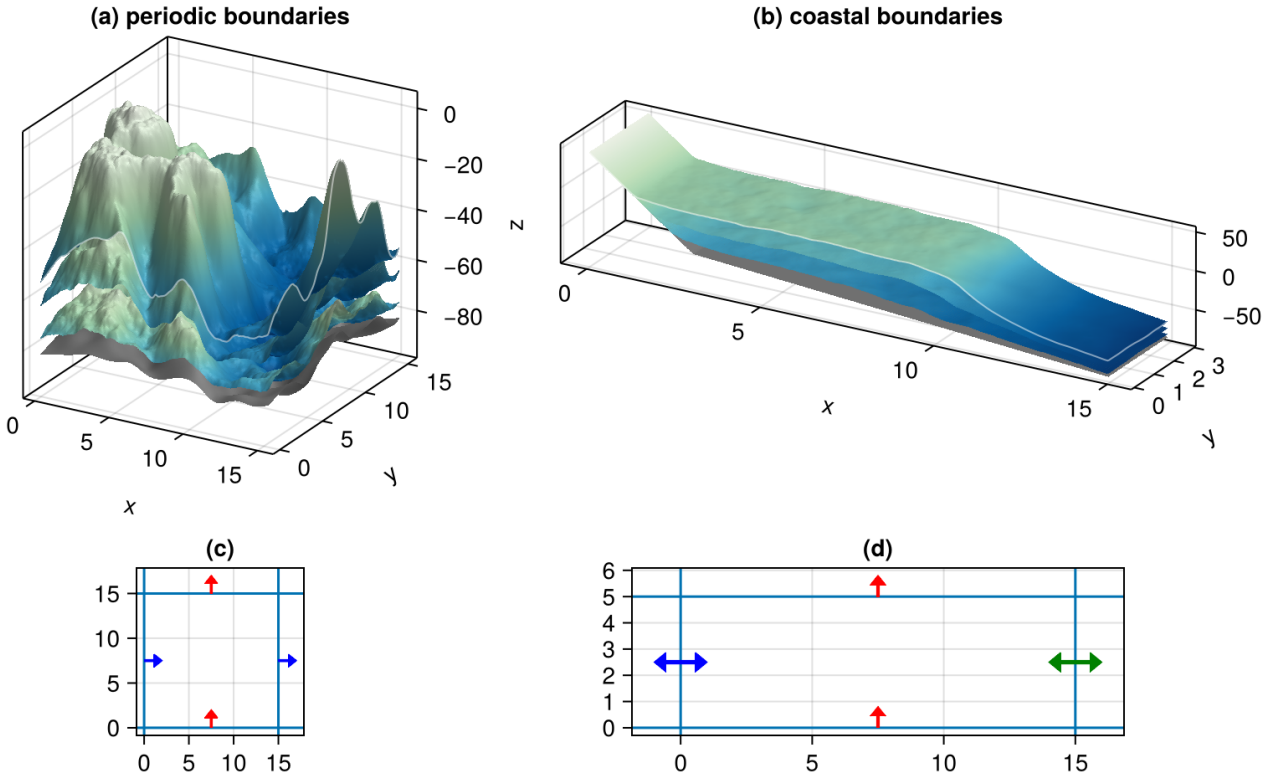

Figure 6. Model topologies. CarboKitten allows the user to choose different topologies for the spatial modelling. In panel (a) we see a group of reef islands that were modelled on a fully periodic grid of size 250×250, using a randomly generated initial topography. A more common use case is shown in panel (b), where the x coordinate is reflected at the boundaries, while the y coordinate is periodic, thus modelling a small strip of coastline. Here the grid size is 250×50, and the initial topography is a linearly declining slope of 0.3% (with the exception of the shore, which is steeper). Panels (c) and (d) schematically illustrate these same box topologies using coloured arrows.

CarboKitten ships with routines for visualisation and data extraction into CSV files. This makes it easier for novice users to use results from CarboKitten in further processing pipelines that rely on other programming languages. Data extracted includes sediment accumulation curves, age-depth models, water depth, and stratigraphic columns with facies code, allowing to test a wide range of hypotheses. These include, but are not limited to, testing hypotheses on orderedness of strata (Burgess, 2016), preservation orbital forcing (Kemp et al., 2016), proxy records (Curtis et al., 2025), or preservation of biotic information such as patterns of origination and extinction, biostratigraphic precision, and evolutionary change (Hohmann and Jarochowska, 2025; Hohmann et al., 2024; Holland and Patzkowsky, 2002).

https://doi.org/10.5194/egusphere-2025-4561
Preprint. Discussion started: 13 October 2025

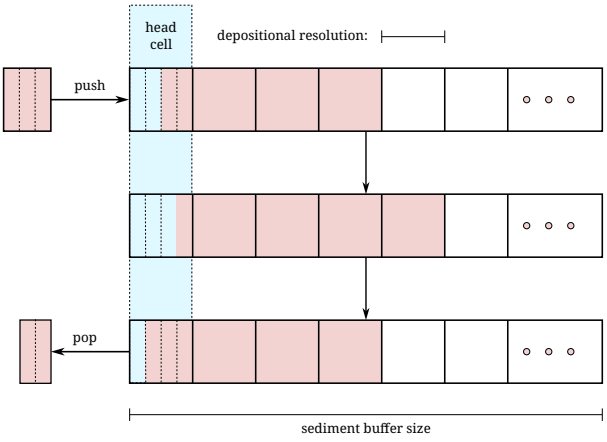

Figure 7. Above we see a buffer. First we push a parcel of size $3/4$, then we pop an amount of $1/2$. This popped parcel will have different fractions from the pushed one, since it also draws from the half filled row that was in the stack before pushing. In this sense, a small amount of facies mixing will take place, depending on the depositional resolution chosen.

4.4 Performance

Since CarboKitten is written in Julia with performance in mind, it should be efficient to run, even on consumer grade hardware, i.e. an average laptop. We are yet to substantiate this claim. Since Julia is a just-in-time compiled language, the first execution of any code in a new session always takes a bit longer than subsequent runs. Measurements presented in this section do not include this initial overhead.

4.4.1 Baseline

Our baseline model is the example included in CarboKitten, grid size 100×50 with 5000 time steps of 200 years each (results shown in Figure 4). This model runs in 27 seconds on a Intel Core i7 at 3.0 GHz.

With regards to memory consumption, CarboKitten allocates a fixed amount of memory at the start of a model run, which scales linearly with the size of the grid. The most significant fraction of the memory is occupied by the sediment buffer. In the example run we have a buffer size of 50. With three facies types being stored this results in an array size of $100 \times 50 \times 50 \times 3$, stored in double precision gives a mere 6MB. However, for a 300×300 sized grid this already increases to 108MB.

4.4.2 Scaling

The run-time and memory consumption of CarboKitten should scale linearly with the number of pixels in the grid, with two complicating factors. Firstly, for smaller models the run-time can become limited by many smaller writes to HDF5. For those cases we provide a method of running models entirely in-memory. The second complication is the transport model. Here run times may vary due to the number of integration steps required for stability reasons. Increasing the resolution of a model also

https://doi.org/10.5194/egusphere-2025-4561
Preprint. Discussion started: 13 October 2025

means increasing the number of transport integration time steps required by the same factor (considering the CFL condition for advective transport). Transport efficiency is also affected by the local topography: increasing the slope also increases the number of integration steps required. Carbonate platforms have the tendency to generate steep slopes due to exponential sedimentation rates in the production model. These steep slopes can be mittigated by setting a diffusion coefficient. On the other hand, modelling on-shore transport due to wave transport can induce steeper slopes, again requiring smaller integration time steps. Note that we are speaking of integration steps of the transport model, which can be any integer fraction of a full model time step. When the transport model needs too many steps for every model step, we can start to question the accuracy of the model as a whole, and the user should try decreasing the time-step of the full model to compensate.

4.4.3 Benchmark

To further quantify these complications in our estimated run-times, we run a model of a single atoll on three different resolutions ($200, 100$, and 50 m, corresponding to grid sizes of $75^2, 150^2, 300^2$) with three different step sizes ($400, 200$, and 100 yr, corresponding to 2500, 5000, and 10000 steps), for a total of nine benchmark cases. We set the interval of the cellular automaton to compensate for the number of time steps. This way, runs with the same grid size should have very similar output. The results are shown in Figure 8.

The combination of 2500 time steps with a 300^2 grid size yields instabilities in the transport model and is left out of the results. Other than that, CarboKitten scaled as predicted from our previous considerations.

4.4.4 Validation

We may validate our benchmark by looking at the results of the runs with grid size 150^2. This is shown in Figure 9. These results show that, when time steps are taken small enough, CarboKitten converges to a consistent result that does not depend on the size of the time step.

4.4.5 Potential for GPU optimisation

At the time of writing, CarboKitten is a single threaded CPU code. However, the structure of the model, is highly ammenable to optimisation on a GPU, which would drastically improve run-times further. Going through the steps of the composed model Section 2.5: the cellular automaton is a stencil operation, production a map, disintegration a stencil, transport is implemented as an iterated stencil, and deposition is a map. Both stencil and map operations are highly localized in memory and are ideal for implementation on a GPU.

4.5 Documentation

CarboKitten is written entirely using literate programming (Knuth, 1984). This means that the implementation of CarboKitten is written as an integral part of its own documentation, using a system called Entangled (Hidding, 2023). The aim is that interested readers have a direct reference to the code implementing the methods that are explained in the documentation.

https://doi.org/10.5194/egusphere-2025-4561
Preprint. Discussion started: 13 October 2025

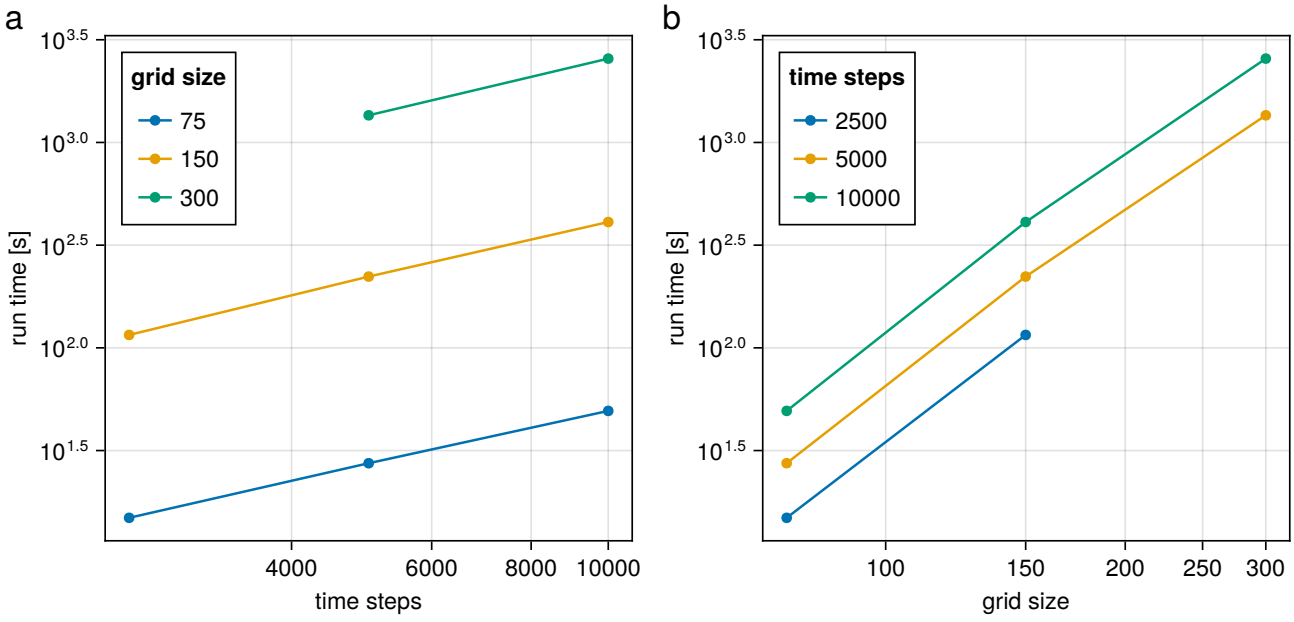

Figure 8. Benchmark with respect to number of time steps and grid size. Panel (a) shows the run-time dependency on the number of time-steps, while panel (b) shows the dependency on the number of grid cells on each axis, both on a log-log scale. This scaling follows the predicted behaviour: linear in both the number of time-steps and total number of grid cells (on this plot being the grid size squared). Note that the run with 2500 time steps and 300^2 grid size is left out, since the transport model was unstable for that configuration. These numbers were consistent throughout multiple runs.

5 Examples

We provide two examples of typical tasks users are likely to undertake: creating a simulation using an empirical, externally provided sea level curve and one with explicit forcing by an insolation curve. These examples are supported by the code used to generate this executable manuscript (FIXME ref to the code) and users are encourage to use that code as a starting point for modifying these examples for their needs.

The third example serves to illustrate the details of how the wave-induced transport is modelled and how modelling decisions and parameter choices affect the outcomes obtained using this feature.

5.1 Sea level

Variables external to the production, which modulate it the most, are the sea level and insolation. The sea level, together with subsidence, result in the *relative* sea level, which translates into *water depth* at any given position in the basin. The sea level must be specified as a function of time. It can be a constant, a continuous function or an empirical dataset. Empirical datasets

https://doi.org/10.5194/egusphere-2025-4561
Preprint. Discussion started: 13 October 2025

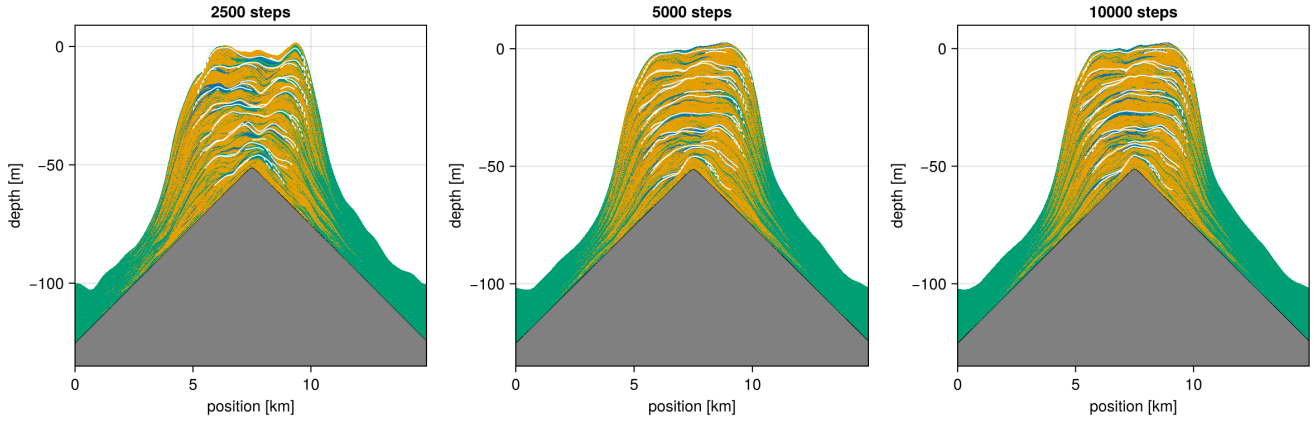

Figure 9. Benchmark validation. This shows a crosssection of the runs with a grid size of 150^2. Looking at the first output, using only 2500 time steps, we see a wave like pattern even where the deep sea facies dominate. These waves are not physical, but a result from taking the time step too large. When we look at the results from 5000 and 10000 time steps, they look so similar that we can conclude that in this case 5000 steps was enough to get accurate results.

can be read in as text files and need to be interpolated to equidistant intervals corresponding to the time step with which the model is run.

The example here uses the sea level curve by Lisiecki and Raymo (2005), reproduced in the compilation by Miller et al. (2005). The dataset of relative sea level records derived from foraminifer $\delta^{18}O$ extracted from this compilation is included in CarboKitten to facilitate simulations of the most typical sea-level scenarios. In this example we start the model at $2\ \mathrm{Ma}$ and build the platform until $134.54\ \mathrm{ka}$, i.e. until the end of the record by Lisiecki and Raymo (2005), using a time step of 200 y.

5.2 Insolation

The relationship between production and insolation can be modified with user-provided parameters. It may be confusing that the extinction coefficient k is, in CarboKitten, a property of the carbonate factory and the facies it deposits and not of the basin or position in it. In reality extinction coefficient varies for different wavelengths of the sunlight spectrum, but the set of its values across the spectrum is constant for a given water body. While different carbonate factories exploit (or ignore, in the case of the aphotic factory) different parts of the light spectrum, the model is agnostic to it and allows users to set k to values that may represent an average across different producers using different wavelengths.

As default, we use insolation of $400\ \mathrm{W/m^2}$, which is approximately equivalent to $2000\ \mathrm{\mu Em^{-2}s^{-1}}$ used by Bosscher and Schlager (1992). This is representative of insolation on the sea surface at midday in the tropics. However, insolation varies with the position of the Earth with respect to the Sun and on geological timescales this variation may affect the patterns of sediment production.

https://doi.org/10.5194/egusphere-2025-4561
Preprint. Discussion started: 13 October 2025

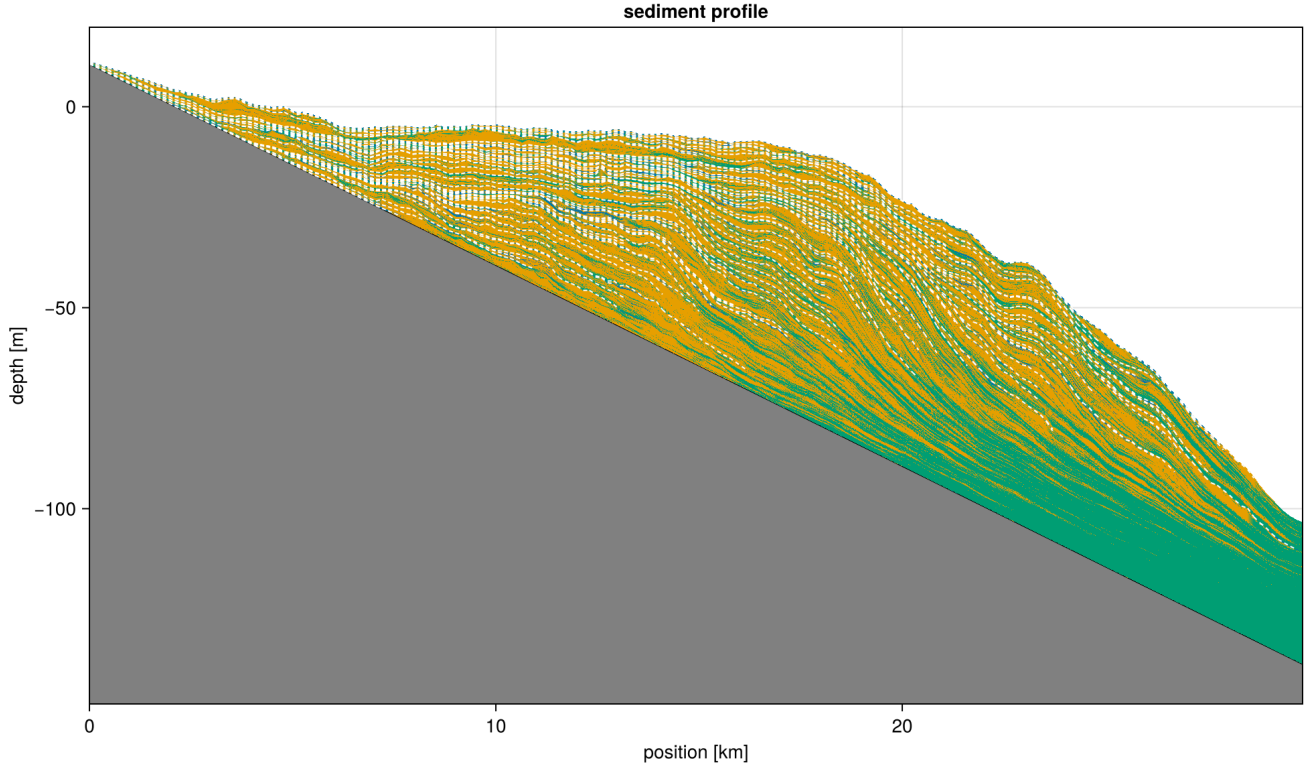

Figure 10. Platform generated using the sea level curve of Lisiecki et al. (2005).

Incoming Solar Radiation can be used as an input vector to modulate production. CarboKitten is agnostic with respect to the source of this information. As an example, here we use the daily mean insolation on June solstice, calculated using the astronomical solution by Laskar (2004), obtained through the R package `palinsol` (Crucifix, 2023). Here we obtain it for the coming million year (starting in 1950, which is when the astronomical solution starts) at the 25° N latitude and use the total solar irradiance value of 1361 $\mathrm{kW m^{-2}}$. Variation in solar irradiance is so small that it would hardly manifest itself if linearly propagated to the sea level curve. A universal transfer function describing the relationship between insolation and sea level does not exist. For the purpose of illustrating the functionality of the model, we calculate the sea level as an amplified insolation value. The amplification is chosen arbitrarily as the square of the insolation anomaly, with the anomaly being the deviation from mean irradiation.

The insolation file can be read into a CarboKitten script defining the model to be run. The alternative is calling R directly from Julia using `RCall.jl`.

5.3 Wave induced transport

We model the transport by waves by setting the velocity v_f and shear s_f components in the transport Equation 7.

https://doi.org/10.5194/egusphere-2025-4561
Preprint. Discussion started: 13 October 2025

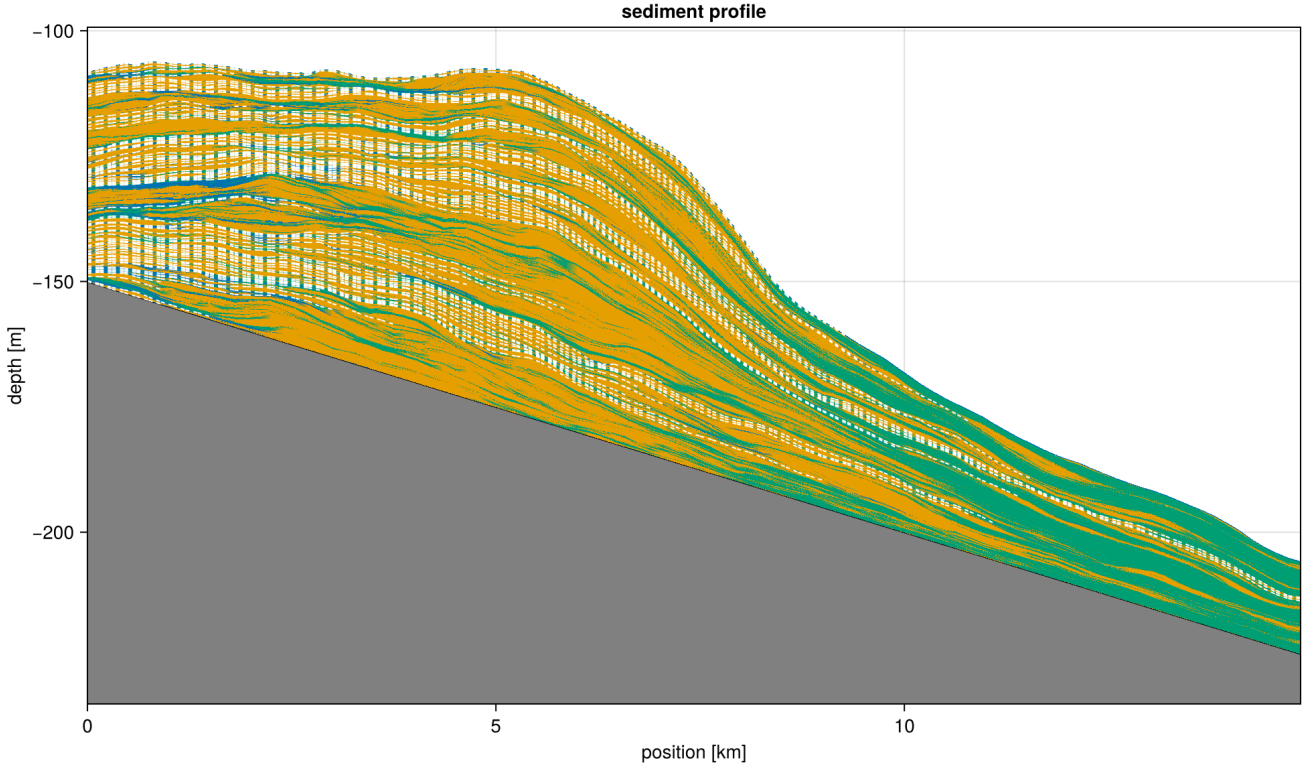

Figure 11. Platform generated using the daily mean insolation during June solstice at the 25° N latitude for a period of 1 Myr starting in 1950 and using a sea level curve obtained by amplifying the insolation values.

Considering the long timescales we are working with, we limit ourselves to a highly simplified model, with the goal of achieving an effect comparable with that of wave-induced transport. Given the timescales for which the model is developed, with time steps of the order of 100 years, a more physical representation of wave-induced transport is not possible. By necessity, the result imitates the time-averaged effect of tranport.

Our approach is illustrated with an example of an atoll, starting with a conical topography and periodic boundaries.

Here we try three different velocity profiles: first no onshore component, second a constant vector that does not depend on water depth, and third an attempt at a more realistic scenario.

The following equation is the well known phase velocity of waves as a function of depth from linear wave theory,

$$v(w) = \sqrt{\frac{\lambda g}{k}} \tanh(kw), \tag{10}$$

https://doi.org/10.5194/egusphere-2025-4561
Preprint. Discussion started: 13 October 2025

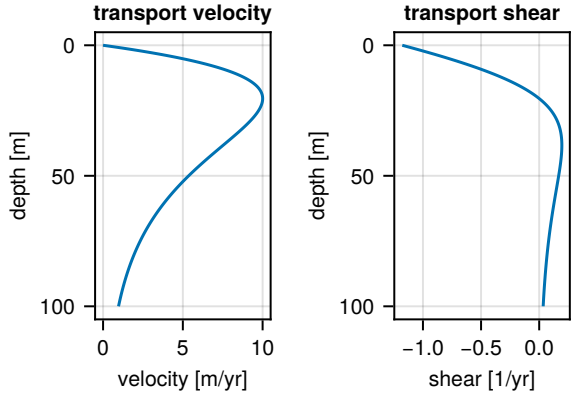

Figure 12. Depth profile of wave velocity and shear. The velocity profile was taylored to have a maximum of $10\ \mathrm{m/yr}$ at a depth of $20\ \mathrm{m}$. Where the shear is negative (assuming transport is directed onshore), there is a net accumulation of sediment.

where w is the water depth, k the wave number ($k = 2\pi/\lambda$), and g is the gravitational acceleration. This velocity is the phase-velocity of surface waves, given the total depth of the water. To evaluate the transport velocity at deeper levels, we multiply the phase velocity with a factor $\exp(-kw)$ to account for Stokes drift:

$$v_f = A_f \exp(-kw)\tanh(kw), \tag{11}$$

where A_f is the facies-dependent maximum transport velocity. The k parameter can be tweaked to set the depth at which the maximum transport velocity is attained. We assume most of the sediment transport happens close to the sea floor. This profile is chosen for its assymptotic properties: at high water depth the transport velocity converges to zero, while the decrease in wave velocity towards shallow depths ensures that there is a net influx of material close to the shore. An example of this profile is shown in Figure 12.

We model the formation of an atoll for three cases: no wave transport, constant transport directed west-ward (along the x-axis), and a depth dependent velocity profile. The results of this experiment are shown in Figure 13. Velocity functions are configured for each facies separately. We found that it was quite easy to create an unstable model by choosing on-shore velocities too high, particularly in the case where the velocity shear is non-zero. Build-up of material due to high on-shore velocity can be compensated by setting a higher facies diffusion coefficient.

If we assume that both the facies specific diffusivity and the wave velocity are both some constant times a hypothetical carrying water velocity, it would be fitting to make sure that for each facies the diffusivity and velocity have a similar proportion. In our experiment we took the values listed in Table 2. It is very hard to find proper motivation for any of these values, but by changing them we can learn more about the mechanisms and systematic behaviours of the model and by extension possibly learn more about the formation of carbonate platforms and study sensitivities in their observed stratigraphic patterns.

https://doi.org/10.5194/egusphere-2025-4561
Preprint. Discussion started: 13 October 2025

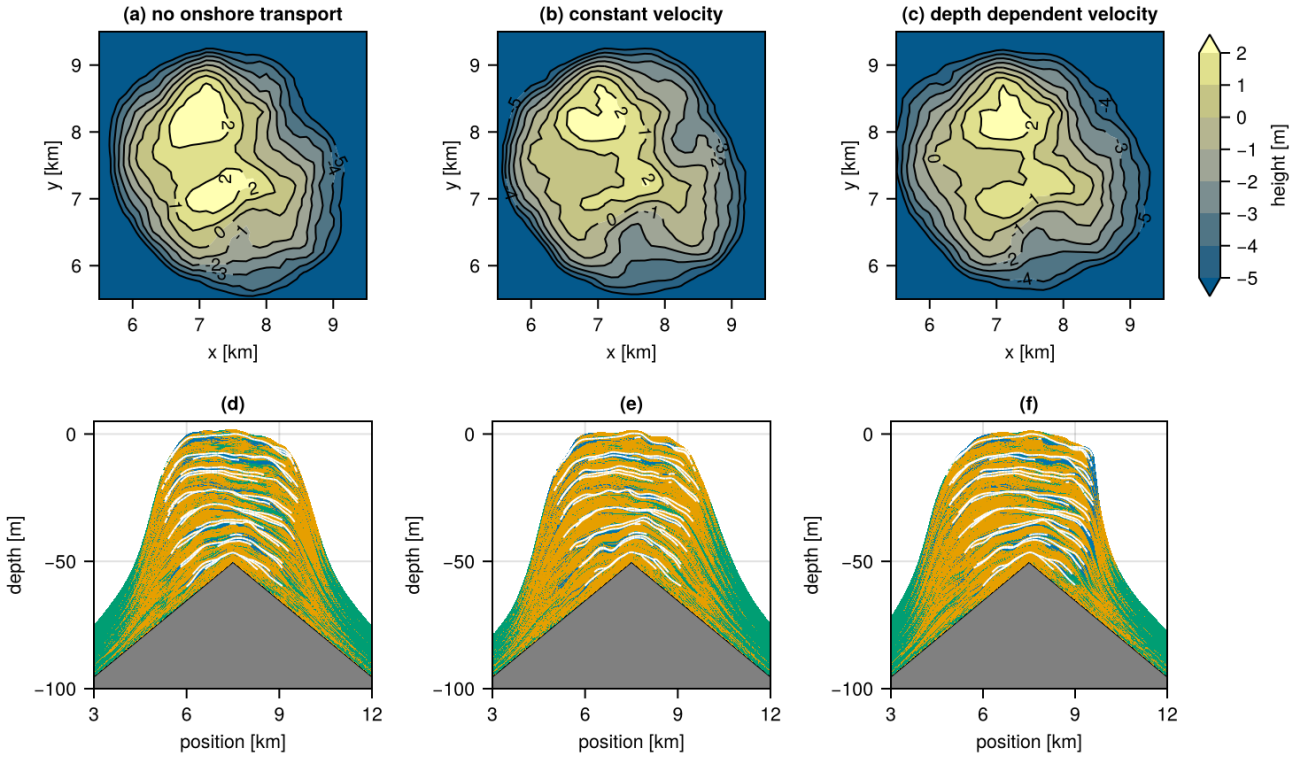

Figure 13. Topography and sediment profiles of an atoll. We ran the same model three times with different on-shore velocity profiles: no on-shore transport, a constant velocity and lastly the profile given in Equation 11. The top row (panels a, b, and c) show the topography of the generated island, while the bottom row (panels d, e, and f) show the corresponding sediment profiles. Small differences in water depth may get amplified exponentially by the production model, so we see some stark differences in the outcomes for the different velocity profiles. Comparing the first (without additional transport vector) and second case (flat profile), we see little change in the overall shape of the atoll, but there is a clear difference in the facies composition at the transition between oligophotic (yellow) and aphotic (green) dominated areas. In the third case we see the topography changed significantly between the leeward and windward sides of the atoll, where the slope is much steeper. Also the facies composition changed further: most notably we see a relative prominence of euphotic (blue) facies on the windward side of the island.

Table 2. chosen parameters to generate results in Figure 13. We used a lithification time of $100\mathrm{yr}$ and a disintegration rate of $50\mathrm{m/Myr}$.

facies	diffusivity $[\mathrm{m/yr}]$	velocity $[\mathrm{m/yr}]$
euphotic	20.0	2.0
oligophotic	10.0	0.5
aphotic	50.0	2.0

https://doi.org/10.5194/egusphere-2025-4561
Preprint. Discussion started: 13 October 2025

6 Conclusions

CarboKitten is a new Open Source stratigraphic forward model dedicated for carbonate depositional environments and modeling of timescales between centuries and millions of years. It integrates previous, well-tested approaches used by the community, i.e. the production model by Bosscher and Schlager (1992) and the generation of spatial heterogeneity proposed by Burgess (2013) with a new approach to sediment transport, based on the concept of the *active layer* by Paola et al. (1992). The software allows modeling and visualization accessible to laptop users, including attractive plotting functions for common use-cases in stratigraphy and sedimentology, such as Wheeler diagrams, age-depth models and stratigraphic columns. CarboKitten uses heuristics to approximate the dynamics of carbonate production, wave transport and biologically driven spatial heterogeneity. The algorithms do not replicate the physical and biological processes behind these phenomena, but allow obtaining results imitating them at timescales at which they cannot be observed directly.

At this stage, CarboKitten's primary value lies not in a realistic replication of empirical stratigraphic architectures, but in its utility for testing hypotheses on the formation of the carbonate geological record and on our own understanding on its governing processes. Further work is needed to allow more detailed reconstructions of known geological situations. Among future refinements are empirical validation of transport and production values or storing the history of sediment transport to track autochthonous and allochthonous sediment.

CarboKitten offers a powerful tool to ground-truth concepts of how time is represented in the physical rock record (e.g., Burgess, 2008; Burgess et al., 2019; Sultana et al., 2022) and constrain the limits of reconstruction of processes such as evolution (Holland and Patzkowsky, 1999; Hannisdal, 2006; Hohmann et al., 2024), climate change, or other aspects of the changing Earth's environment (e.g., Kemp et al., 2016; Kemp and Van Manen, 2019; Myrow and Grotzinger, 2000; Geyman et al., 2021; Husinec et al., 2023; Curtis et al., 2025). We hope the accessibility and reproducibility of CarboKitten simulations will encourage wider use of stratigraphic forward models towards a hypothetico-deductive research in stratigraphy.

Code availability. CarboKitten is available under the GNU Public Licencse 3.0 and is hosted on Github. Releases are also made available on Zenodo (doi:10.5281/zenodo.14051612), see Hidding et al. (2025).

Author contributions. EJ, JH, PB and NH conceptualized the study. Software and visualizations were developed by JH with contributions from EJ, XL, NH, and HS. All authors contributed to the methodology. EJ was responsible for funding acquisition and project administration. JH and EJ drafted the manuscript and PB and NH contributed to the final version.

Competing interests. The authors declare that they have no conflict of interest.

https://doi.org/10.5194/egusphere-2025-4561
Preprint. Discussion started: 13 October 2025

Acknowledgements. We thank Joris Eggenhuisen for discussions on the transport model and Charlotte Summers for programming support. Niels Drost provided administrative and management support during the project.

Funded by the European Union (ERC, MindTheGap, StG project no 101041077). Views and opinions expressed are however those of the author(s) only and do not necessarily reflect those of the European Union or the European Research Council. Neither the European Union nor the granting authority can be held responsible for them.

https://doi.org/10.5194/egusphere-2025-4561
Preprint. Discussion started: 13 October 2025

References

Adams, E. W. and Schlager, W.: Basic Types of Submarine Slope Curvature, Journal of Sedimentary Research, 70, 814–828, https://doi.org/10.1306/2DC4093A-0E47-11D7-8643000102C1865D, 2000.

Barrett, S. J. and Webster, J. M.: Reef Sedimentary Accretion Model (ReefSAM): Understanding coral reef evolution on Holocene time scales using 3D stratigraphic forward modelling, Marine Geology, 391, 108–126, https://doi.org/10.1016/j.margeo.2017.07.007, 2017.

Bosscher, H. and Schlager, W.: Computer simulation of reef growth, Sedimentology, 39, 503–512, 1992.

Bosscher, H. and Southam, J.: CARBPLAT—A computer model to simulate the development of carbonate platforms, Geology, 20, 235–238, https://doi.org/10.1130/0091-7613(1992)020<0235:CACMTS>2.3.CO;2, 1992.

Burgess, P. M.: The nature of shallow-water carbonate lithofacies thickness distributions, Geology, 36, 235–238, https://doi.org/10.1130/G243326A.1, 2008.

Burgess, P. M.: CarboCAT: A cellular automata model of heterogeneous carbonate strata, Computers & geosciences, 53, 129–140, 2013.

Burgess, P. M.: Identifying Ordered Strata: Evidence, Methods, and Meaning, Journal of Sedimentary Research, 86, 148–167, https://doi.org/10.2110/jsr.2016.10, 2016.

Burgess, P. M., Wright, V. P., and Emery, D.: Numerical forward modelling of peritidal carbonate parasequence development: implications for outcrop interpretation, Basin Research, 13, 1–16, https://doi.org/10.1046/j.1365-2117.2001.00130.x, 2001.

Burgess, P. M., Masiero, I., Toby, S. C., and Duller, R. A.: A big fan of signals? Exploring autogenic and allogenic process and product in a numerical stratigraphic forward model of submarine-fan development, Journal of Sedimentary Research, 89, 1–12, https://doi.org/10.2110/jsr.2019.3, 2019.

Crucifix, M.: palinsol: Insolation for Palaeoclimate Studies, https://doi.org/10.32614/CRAN.package.palinsol, 2023.

Curtis, A., Bloem, H., Wood, R., Bowyer, F., Shields, G. A., Zhou, Y., Yilales, M., and Tetzlaff, D.: Natural sampling and aliasing of marine geochemical signals, Scientific Reports, 15, 760, https://doi.org/10.1038/s41598-024-84871-6, 2025.

Danisch, S. and Krumbiegel, J.: Makie.jl: Flexible high-performance data visualization for Julia, Journal of Open Source Software, 6, 3349, https://doi.org/10.21105/joss.03349, 2021.

Demicco, R. V.: CYCOPATH 2D—a two-dimensional, forward model of cyclic sedimentation on carbonate platforms, Computers & Geosciences, 24, 405–423, https://doi.org/10.1016/S0098-3004(98)00024-7, 1998.

Ding, X., Salles, T., Flament, N., and Rey, P.: Quantitative stratigraphic analysis in a source-to-sink numerical framework, Geoscientific Model Development, 12, 2571–2585, https://doi.org/10.5194/gmd-12-2571-2019, 2019.

Drummond, C. N. and Dugan, P. J.: Self-organizing models of shallow-water carbonate accumulation, Journal of Sedimentary Research, 69, 939–946, https://doi.org/10.2110/jsr.69.939, 1999.

Dyer, B., Maloof, A. C., Purkis, S. J., and Harris, P. M. M.: Quantifying the relationship between water depth and carbonate facies, Sedimentary Geology, 373, 1–10, https://doi.org/10.1016/j.sedgeo.2018.05.011, 2018.

Falivene, O., Frascati, A., Bolla Pittaluga, M., and Martin, J.: Three-dimensional Reduced-Complexity Simulation of Fluvio-Deltaic Clastic Stratigraphy, Journal of Sedimentary Research, 89, 46–65, https://doi.org/10.2110/jsr.2018.73, 2019.

Geyman, E. C., Maloof, A. C., and Dyer, B.: How is sea level change encoded in carbonate stratigraphy?, Earth and Planetary Science Letters, 560, 116 790, https://doi.org/10.1016/j.epsl.2021.116790, 2021.

Granjeon, D. and Joseph, P.: Concepts and Applications of A 3-D Multiple Lithology, Diffusive Model in Stratigraphic Modeling, in: Numerical Experiments in Stratigraphy: Recent Advances in Stratigraphic and Sedimentologic Computer Simulations, edited by Harbaugh,

https://doi.org/10.5194/egusphere-2025-4561
Preprint. Discussion started: 13 October 2025

J. W., Watney, W. L., Rankey, E. C., Slingerland, R., Goldstein, R. H., and Franseen, E. K., vol. 62, pp. 197–209, SEPM (Society for Sedimentary Geology), https://doi.org/10.2110/pec.99.62.0197, 1999.

Hannisdal, B.: Phenotypic evolution in the fossil record: numerical experiments, The Journal of Geology, 114, 133–153, https://doi.org/10.1086/499569, 2006.

Hidding, J.: Entangled, a Bidirectional System for Sustainable Literate Programming, in: 2023 IEEE 19th International Conference on e-Science (e-Science), pp. 1–9, https://doi.org/10.1109/e-Science58273.2023.10254816, 2023.

Hidding, J., Jarochowska, E., Liu, X., Burgess, P., Hohmann, N., and Spreeuw, H.: CarboKitten.jl, https://doi.org/10.5281/zenodo.15742533, 2025.

Hill, J., Tetzlaff, D., Curtis, A., and Wood, R.: Modeling shallow marine carbonate depositional systems, Computers & Geosciences, 35, 1862–1874, https://doi.org/10.1016/j.cageo.2008.12.006, 2009.

Hohmann, N. and Jarochowska, E.: StratPal: An R package for creating stratigraphic paleobiology modelling pipelines, Methods in Ecology and Evolution, 16, 678–686, https://doi.org/https://doi.org/10.1111/2041-210X.14507, 2025.

Hohmann, N., Koelewijn, J. R., Burgess, P., and Jarochowska, E.: Identification of the mode of evolution in incomplete carbonate successions, BMC Ecology and Evolution, 24, 113, https://doi.org/10.1186/s12862-024-02287-2, 2024.

Holland, S. M.: The quality of the fossil record: A sequence stratigraphic perspective, Paleobiology, 26, 148–168, https://doi.org/10.1017/S0094837300026919, 2000.

Holland, S. M. and Patzkowsky, M. E.: Models for simulating the fossil record, Geology, 27, 491–494, https://doi.org/10.1130/0091-7613(1999)027<0491:MFSTFR>2.3.CO;2, 1999.

Holland, S. M. and Patzkowsky, M. E.: Stratigraphic Variation in the Timing of First and Last Occurrences, PALAIOS, 17, 134–146, https://doi.org/10.1669/0883-1351(2002)017<0134:SVITTO>2.0.CO;2, 2002.

Husinec, A., Read, J. F., and Kemp, D. B.: Orbital forcing of Upper Jurassic (Tithonian) shallow-water carbonates, Tethyan Adriatic Platform, Croatia evaluated using synthetic vs. real data sets, Palaeogeography, Palaeoclimatology, Palaeoecology, 622, 111 617, https://doi.org/10.1016/j.palaeo.2023.111617, 2023.

Hutton, E. W. H. and Syvitski, J. P. M.: *Sedflux 2.0*: An advanced process-response model that generates three-dimensional stratigraphy, Computers & Geosciences, 34, 1319–1337, https://doi.org/10.1016/j.cageo.2008.02.013, 2008.

James, S. C., Jones, C. A., Grace, M. D., and Roberts, J. D.: Advances in sediment transport modelling, Journal of Hydraulic Research, 48, 754–763, 2010.

Jean Borgomano, C. L., Lanteaume, C., Léonide, P., Fournier, F., Montaggioni, L. F., and Masse, J.-P.: Quantitative carbonate sequence stratigraphy: Insights from stratigraphic forward models, AAPG Bulletin, 104, 1115–1142, https://doi.org/10.1306/11111917396, 2020.

Kemp, D. B. and Van Manen, S. M.: Metre-scale cycles in shallow water carbonate successions: Milankovitch and stochastic origins, Sedimentology, 66, 2590–2604, https://doi.org/10.1111/sed.12609, 2019.

Kemp, D. B., Van Manen, S. M., Pollitt, D. A., and Burgess, P. M.: Investigating the preservation of orbital forcing in peritidal carbonates, Sedimentology, 63, 1701–1718, https://doi.org/10.1111/sed.12282, 2016.

Kemp, D. B., Fraser, W. T., and Izumi, K.: Stratigraphic completeness and resolution in an ancient mudrock succession, Sedimentology, 65, 1875–1890, https://doi.org/10.1111/sed.12450, 2018.

Kenter, J. A. M.: Carbonate platform flanks: slope angle and sediment fabric, Sedimentology, 37, 777–794, https://doi.org/https://doi.org/10.1111/j.1365-3091.1990.tb01825.x, 1990.

Knuth, D. E.: Literate Programming, The Computer Journal, 27, 97–111, https://doi.org/10.1093/comjnl/27.2.97, 1984.

https://doi.org/10.5194/egusphere-2025-4561
Preprint. Discussion started: 13 October 2025

Laskar, J.: A long-term numerical solution for the insolation quantities of the Earth, Astronomy & Astrophysics, 428, 261–285, https://doi.org/10.1051/0004-6361:20041335, 2004.

Lisiecki, L. E. and Raymo, M. E.: A Pliocene-Pleistocene stack of 57 globally distributed benthic δ18O records, Paleoceanography, 20, https://doi.org/10.1029/2004PA001071, 2005.

Liu, J. and Liu, K.: Estimating stratal completeness of carbonate deposition via process-based stratigraphic forward modeling, Science China Earth Sciences, 64, 253–259, https://doi.org/10.1007/s11430-020-9660-8, 2021.

Liu, J., Webster, J. M., Salles, T., Wang, S., Ma, Y., Xu, W., Li, G., and Yan, W.: The Formation of Atolls: New Insights From Numerical Simulations, Journal of Geophysical Research: Earth Surface, 127, e2022JF006 812, https://doi.org/10.1029/2022JF006812, 2022.

Masiero, I., Kozlowski, E., Antonatos, G., Xi, H., and Burgess, P.: Numerical stratigraphic forward models as conceptual knowledge repositories and experimental tools: An example using a new enhanced version of CarboCAT, Computers & Geosciences, 138, 104 453, https://doi.org/10.1016/j.cageo.2020.104453, 2020.

Masiero, I., Burgess, P., Hollis, C., Manifold, L., Gawthorpe, R., Lecomte, I., Marshall, J., and Rotevatn, A.: Syn-rift carbonate platforms in space and time: testing and refining conceptual models using stratigraphic and seismic numerical forward modelling, in: Seismic Characterization of Carbonate Platforms and Reservoirs, edited by Hendry, J., Burgess, P., Hunt, D., Janson, X., and Zampetti, V., p. 0, Geological Society of London, ISBN 978-1-78620-539-1, https://doi.org/10.1144/SP509-2019-217, 2021.

Miller, K. G., Kominz, M. A., Browning, J. V., Wright, J. D., Mountain, G. S., Katz, M. E., Sugarman, P. J., Cramer, B. S., Christie-Blick, N., and Pekar, S. F.: The Phanerozoic Record of Global Sea-Level Change, Science, 310, 1293–1298, https://doi.org/10.1126/science.1116412, 2005.

Myrow, P. M. and Grotzinger, J. P.: Chemostratigraphic Proxy Records: Forward Modeling the Effects of Unconformities, Variable Sediment Accumulation Rates, and Sampling-Interval Bias, in: Carbonate Sedimentation and Diagenesis in the Evolving Precambrian World, edited by Grotzinger, J. P. and James, N. P., vol. 67, p. 0, SEPM Society for Sedimentary Geology, ISBN 978-1-56576-189-6, https://doi.org/10-2110/pec.00.67, 2000.

Paola, C., Heller, P. L., and Angevine, C. L.: The large-scale dynamics of grain-size variation in alluvial basins, 1: Theory, Basin research, 4, 73–90, 1992.

Paterson, R. J., Whitaker, F. F., Jones, G. D., Smart, P. L., Waltham, D., and Felce, G.: Accommodation and Sedimentary Architecture of Isolated Icehouse Carbonate Platforms: Insights from Forward Modeling with CARB3D+, Journal of Sedimentary Research, 76, 1162–1182, https://doi.org/10.2110/jsr.2006.113, 2006.

Purkis, S. J., Koppel, J. v. d., and Burgess, P. M.: Spatial self-organization in carbonate depositional environments, SEPM Special Publications, 106, 53–66, https://doi.org/10.2110/sepmsp.106.02, 2016.

Salles, T.: Badlands: A parallel basin and landscape dynamics model, SoftwareX, 5, 195–202, https://doi.org/10.1016/j.softx.2016.08.005, 2016.

Salles, T., Ding, X., and Brocard, G.: pyBadlands: A framework to simulate sediment transport, landscape dynamics and basin stratigraphic evolution through space and time, PLOS ONE, 13, e0195 557, https://doi.org/10.1371/journal.pone.0195557, 2018.

Schlager, W. and Camber, O.: Submarine slope angles, drowning unconformities, and self-erosion of limestone escarpments, Geology, 14, 762–765, https://doi.org/10.1130/0091-7613(1986)14<762:SSADUA>2.0.CO;2, 1986.

Schlager, W. and Warrlich, G.: Record of sea-level fall in tropical carbonates, Basin Research, 21, 209–224, https://doi.org/10.1111/j.1365-2117.2008.00383.x, 2009.

https://doi.org/10.5194/egusphere-2025-4561
Preprint. Discussion started: 13 October 2025

Strobel, J., Cannon, R., Christopher, G. S., Kendall, C. S., Biswas, G., and Bezdek, J.: Interactive (SEDPAK) simulation of clastic and carbonate sediments in shelf to basin settings, Computers & Geosciences, 15, 1279–1290, https://doi.org/10.1016/0098-3004(89)90092-7, 1989.

Sultana, D., Burgess, P., and Bosence, D.: How do carbonate factories influence carbonate platform morphology? Exploring production-transport interactions with numerical forward modelling, Sedimentology, 69, 372–393, https://doi.org/10.1111/sed.12943, 2022.

Sylvester, Z., Straub, K. M., and Covault, J. A.: Stratigraphy in space and time: A reproducible approach to analysis and visualization, Earth-Science Reviews, 250, 104 706, https://doi.org/10.1016/j.earscirev.2024.104706, 2024.

Tetzlaff, D.: Stratigraphic forward modeling software package for research and education, https://doi.org/10.48550/arXiv.2302.05272, 2023.

Warrlich, G., Bosence, D., Waltham, D., Wood, C., Boylan, A., and Badenas, B.: 3D stratigraphic forward modelling for analysis and prediction of carbonate platform stratigraphies in exploration and production, Marine and Petroleum Geology, 25, 35–58, https://doi.org/https://doi.org/10.1016/j.marpetgeo.2007.04.005, 2008.

Warrlich, G.-M. D.: 3D computer forward modelling of carbonate platform evolution., Ph.D. thesis, Royal Holloway, University of London, 2000.

Warrlich, G. M. D., Waltham, D. A., and Bosence, D. W. J.: Quantifying the sequence stratigraphy and drowning mechanisms of atolls using a new 3-D forward stratigraphic modelling program (CARBONATE 3D), Basin Research, 14, 379–400, https://doi.org/10.1046/j.1365-2117.2002.00181.x, 2002.

Weij, R., Reijmer, J. J. G., Eberli, G. P., and Swart, P. K.: The limited link between accommodation space, sediment thickness, and inner platform facies distribution (Holocene–Pleistocene, Bahamas), The Depositional Record, 5, 400–420, https://doi.org/10.1002/dep2.50, 2019.

Wild, T. B., Loucks, D. P., and Annandale, G. W.: SedSim: A River Basin Simulation Screening Model for Reservoir Management of Sediment, Water, and Hydropower, Journal of Open Research Software, 7, https://doi.org/10.5334/jors.261, 2019.

Xi, H. and Burgess, P. M.: The stratigraphic significance of self-organization: Exploring how autogenic processes can generate cyclical carbonate platform strata, Sedimentology, 69, 1769–1788, https://doi.org/10.1111/sed.12974, 2022.

Zimmt, J. B., Holland, S. M., Finnegan, S., and Marshall, C. R.: Recognizing pulses of extinction from clusters of last occurrences, Palaeontology, 64, 1–20, https://doi.org/10.1111/pala.12505, 2021.